MEASURING OMEGA INDEPENDENT OF GALAXY BIASING

Avishai Dekel
Racah Institute of Physics, The Hebrew University, jerusalem 91904, Israel.

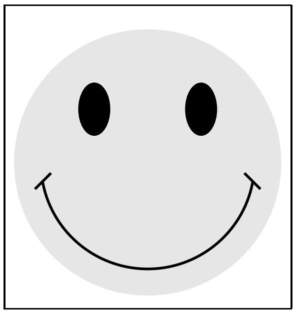

Abstract

I describe methods for measuring the cosmological density parameter Ω from the large-scale peculiar velocity field *independent* of galaxy biasing and Λ. Several such methods assume Gaussian initial fluctuations; they use either the velocity field near a void, or the skewness of the probability distribution of $\boldsymbol{\nabla}\cdot\boldsymbol{v}$, or the initial density fluctuations. All yield $\Omega > 0.3$ with $> 95\%$ confidence.

A new determination is based on comparing the power spectrum of *mass* density fluctuations as derived from the observed velocities with the large-angle fluctuations in the microwave background observed by COBE. For an inflation-motivated flat cosmology with $\Omega + \Lambda = 1$ and cold dark matter, it is found that if the initial fluctuation power index is $n = 1$, maximum likelihood is at $\Omega \simeq (0.7 \pm 0.2)\, h_{50}^{-1.2}$. If $\Omega = 1$, then with no tensor fluctuations $n \simeq (0.8 \pm 0.1) h_{50}^{-0.8}$, and with tensor fluctuations $n \simeq (0.9 \pm 0.1) h_{50}^{-0.8}$.

1 Introduction

Three general kinds of data are used in the effort to determine the cosmological density parameter Ω from large-scale structure: (a) the distribution of galaxies on the sky and in redshift surveys, (b) the large-angle fluctuations in the microwave background (CMB), and (c) the peculiar velocities of galaxies.

As illustrated in Figure 1, these data can be combined to constrain Ω in several different ways. All the methods that use the spatial distribution of galaxies must depend on the unknown relation between the density fluctuations of galaxies and mass, commonly characterized by a linear *biasing* factor b. In the linear approximation to gravitational instability (GI), which is roughly valid for the fields when they are smoothed on large scales, what is actually being measured by these methods is the degenerate parameter $\beta \equiv f(\Omega)/b$ (where $f \approx \Omega^{0.6}$) rather

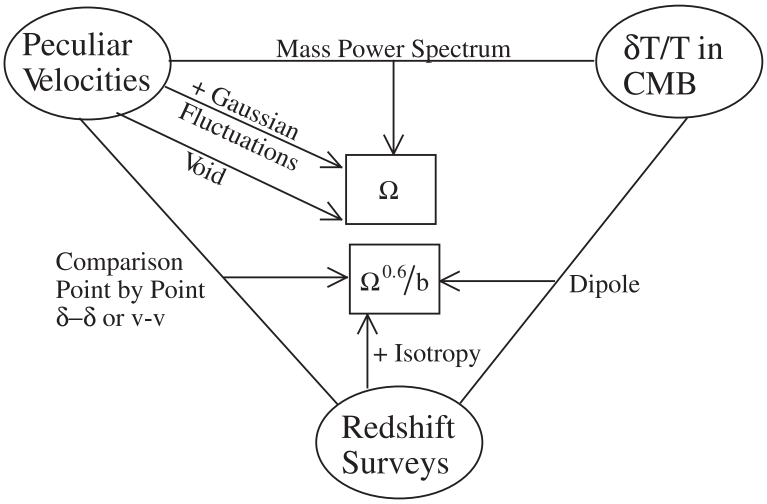

Figure 1: Methods for measuring Ω and β from large-scale observations.

than Ω itself. These methods, reviewed in [18] and [49], include (a) comparisons of the CMB dipole with the acceleration of the Local Group (LG) as predicted via the gravity induced by the galaxy distribution around us, (b) comparisons of the observed peculiar velocities with the galaxy distribution and the predicted velocities deduced from redshift surveys, and (c) measurements of redshift-space distortions under the assumption of global isotropy. The most recent estimates of β for optical and IRAS galaxies lie in the range $0.5 \leq \beta \leq 1$. As argued in §2, the contamination by biasing introduces a significant uncertainty in the translation of the various β measurements to a reliable estimate of Ω.

It is therefore worth considering here alternative methods for determining Ω, which are *independent* of galaxy biasing. These methods are based on the observed peculiar velocities described in §3. One family of such methods uses the velocity data alone, combined with the assumption (supported by observations, e.g. [44]) that the initial fluctuations were drawn from a *Gaussian* random field. Three examples are described in §4: using the velocity field around *voids*, using the *skewness* of $\boldsymbol{\nabla}\cdot\boldsymbol{v}$, and recovering the *initial* probability distribution of density fluctuations.

Another way of determining Ω is based on comparing the observed velocities with the large-angle fluctuations in the *CMB*. Recent comparisons of this sort, via the mass-fluctuation *power spectrum*, are described in §5. These direct estimates of Ω are discussed in §6 in the general context of other cosmological parameters.

2 Uncertainties due to Galaxy Biasing

Galaxy "biasing" clearly exists. The fact that galaxies of different types cluster differently [26] imply that at least some do not trace the underlying mass, and any physical theory would predict non-trivial biasing ([3], [17], [24], [22], [10], [51]). Indeed, simulations of galaxy formation involving gas dynamics ([12], [13]) indicate a biasing relation that is nonlinear in density and is varying with scale. It is therefore not surprising that the various estimates of β show a large scatter. Some of this scatter is due to the different types of galaxies involved, and some may be due to unaccounted for effects of nonlinear gravity or other systematic errors, but a significant fraction of the scatter is likely to reflect non-trivial properties of the biasing scheme. All this means that translating a measured β into Ω is non-trivial; it requires a detailed knowledge of the relevant biasing scheme.

In order to strengthen this point, I demonstrate here that an obvious source of scatter in β is a straightforward consequence of the inevitable *statistical* scatter in the biasing process. Let $\delta(\boldsymbol{x})$ be the field of mass-density fluctuations smoothed at a given scale, and let $\delta_G(\boldsymbol{x})$ be the corresponding field for galaxies of a given type. Treat them as random fields, both with probability densities of zero mean by definition. Denote $\langle\delta^2\rangle \equiv \sigma^2$ and $\langle\delta^3\rangle \equiv S$. Consider the "biasing" relation between galaxies and mass to be a *random* process, specified by the *conditional probability* function $B(\delta_G|\delta)$ [21]. The common deterministic biasing relation, $\delta_G = b(\delta)\delta$, is replaced by the conditional mean,

$$\langle\delta_G|\delta\rangle \equiv b(\delta)\delta. \tag{1}$$

The statistical character of the relation is expressed by the conditional moments of higher order about the mean, such as

$$\langle(\delta_G - b\delta)^2|\delta\rangle \equiv \sigma_b^2, \quad \text{and} \quad \langle(\delta_G - b\delta)^3|\delta\rangle \equiv S_b. \tag{2}$$

This statistical nature of biasing leads to a different "biasing parameter" for each specific application.

Take for example the ratio of variances, $b_2^2 \equiv \langle\delta_G^2\rangle/\langle\delta^2\rangle$, such as being obtained by a ratio of power spectra or two-point correlation functions, or by comparing the mass function of clusters to the variance of δ_G at $8\,\mathrm{h}^{-1}$Mpc [?]. One can prove in general that $\langle\delta_G^m\rangle = \langle\, \langle\delta_G^m|\delta\rangle_{\delta_G}\, \rangle_\delta$, and therefore, $\langle\delta_G^2\rangle = \langle b^2(\delta)\,\delta^2\rangle + \langle\sigma_b^2(\delta)\rangle$. Thus, in the simple case where $b(\delta)$ is constant, b_2 is an overestimate of b by

$$b_2 = b\,(1+\Delta_2)^{1/2}, \quad \Delta_2 \equiv \langle\sigma_b^2\rangle/(\sigma^2 b^2). \tag{3}$$

Another common way of estimating β is via linear regression of the noisy field $-\boldsymbol{\nabla}\cdot\boldsymbol{v}(\boldsymbol{x})$ $[\approx f(\Omega)\delta(\boldsymbol{x})]$ on $\delta_G(\boldsymbol{x})$, or via a regression of the corresponding velocities. The slope of the forward regression of δ_G on δ is $b_f = \langle\delta_G\delta\rangle/\langle\delta^2\rangle$, and the slope of the inverse regression of δ on δ_G is $b_i^{-1} = \langle\delta\delta_G\rangle/\langle\delta_G^2\rangle$. In the case where b is constant, $b_f = b$, and b_i is an overestimate,

$$b_i = b\,(1+\Delta_2). \tag{4}$$

Similarly, most methods for determining β lead to an underestimate.

The level of the effect depends on the actual values of Δ_2 and similar parameters. For example, a goodness of fit test of the $12\,\mathrm{h}^{-1}$Mpc-smoothed density fields of POTENT mass and optical galaxies [31] yields $\chi^2 \sim 2$ per degree of freedom, instead of ~ 1, unless one adds to the assumed errors a biasing scatter of $\sigma_b \sim 0.15$, corresponding to $\Delta_2 \sim 0.25$ (with $\sigma \sim 0.3$ and $b \sim 1$). Alternatively, hydro simulations [13] yield $\sigma_b = 0.25$ under $10\,\mathrm{h}^{-1}$Mpc Gaussian smoothing, i.e. $\Delta_2 \sim 0.4$ (with $\sigma \sim 0.4$). If $b = \Omega = 1$, then the β values derived by the various methods are expected to span the range $0.7 \le \beta \le 1$ just due to the dispersion in the biasing relation. A large skewness in $B(\delta_G|\delta)$ may stretch this range even further.

The moral from the biasing uncertainty is that methods for measuring Ω independent of biasing are desirable.

3 Peculiar Velocity Field

3.1 Data: Mark III

Galaxy distances r_i are estimated by the Tully-Fisher (TF) method for spirals, and by the analogous $D_n - \sigma$ method for ellipticals and SO's. Given a galaxy redshift z_i, the radial peculiar velocity is $u_i = cz_i - r_i$ (H_0 is set to unity; distances are measured in $\mathrm{km\,s^{-1}}$). Several such samples have accumulated in recent years. Assuming that all galaxies trace the same underlying velocity field, the analysis of large-scale motions greatly benefits from merging the different samples into one self-consistent catalog. The recent Mark III catalog ([53], [54], [55]) combines 544 early type galaxies (mostly [38]) with $\sim$2850 spirals ([1], [29], [40], [30], [52], [15], [39]).

The observers differ in their selection procedures, the quantities they measure, the methods of measurement and the TF calibration techniques, which cause systematic errors and made the merger of Mark III non-trivial, along the following steps. (a) Standardizing the selection criteria, *e.g.* rejecting galaxies of high inclination or low rotation, which are suspect of large errors, and sharpening any z cutoff. (b) Rederiving a provisional TF calibration for each data set using an algorithm that simultaneously groups, fits and corrects for selection bias, and then verifying that inverse-TF distances to clusters are similar to the forward-TF distances. (c) Starting with one data set, adding each new set in succession using the galaxies in common to adjust the TF parameters of the new set if necessary. (d) Using only one measurement per galaxy even if it was observed by more than one observer to ensure well defined errors, and using multiple observations for a "cluster" only if the overlap is small (*e.g.* $<50\%$). (e) Adding the ellipticals from Mark II [11], allowing for a slight zero-point shift. Such a careful calibration and merger procedure is *crucial* for reliable results — in several cases it produced TF distances substantially different from those quoted by the original authors. The Mark III catalog enables a reasonable recovery of the dynamical fields with $\sim 12\,\mathrm{h^{-1}Mpc}$ smoothing in a sphere of radius $\sim 60\,\mathrm{h^{-1}Mpc}$ about the LG, extending to $\sim 80\,\mathrm{h^{-1}Mpc}$ in certain regions.

3.2 POTENT Analysis

Given the sparsely-sampled radial velocities u_i, POTENT first computes a *smoothed* radial-velocity field in a spherical grid, $u(\boldsymbol{x})$, using a tensor window function corresponding to a Gaussian window of radius $12\,\mathrm{h^{-1}Mpc}$ ([19], [6], [18]). Weighting inversely by the local density near each object mimics equal-volume averaging that minimizes the bias due to non-uniform sampling, and weighting inversely by the distance errors, σ_i^2, reduces their random effects.

The 3D velocity field is recovered under the assumption of *potential* flow: $\boldsymbol{v}(\boldsymbol{x}) = -\boldsymbol{\nabla}\Phi(\boldsymbol{x})$ [**?**]. According to linear GI, any vorticity mode decays in time as the universe expands, and based on Kelvin's circulation theorem the flow remains vorticity-free in the mildly-nonlinear regime as long as the flow is laminar. The velocity potential can therefore be calculated by integrating the radial velocity along radial rays, $\Phi(\boldsymbol{x}) = -\int_0^r u(r', \theta, \phi)dr'$. Differentiating Φ in the transverse directions then recovers the two missing velocity components.

The underlying mass-density fluctuation field, $\delta(\boldsymbol{x})$, is computed by the approximation [43]

$$\delta_c(\boldsymbol{x}) = \| I - f(\Omega)^{-1} \partial \boldsymbol{v} / \partial \boldsymbol{x} \| - 1 \ , \tag{5}$$

where the bars denote the Jacobian determinant, and I is the unit matrix. This is the solution to the continuity equation under the Zel'dovich assumption that particle displacements evolve in a universal rate, and it reduces to the familiar $\delta = -f^{-1}\boldsymbol{\nabla}\cdot\boldsymbol{v}$ in the linear regime. It approximates the true density in N-body simulations of Gaussian initial conditions, with an *rms* error less than 0.1 over the range $-0.8 \le \delta \le 4.5$.

The results suffer from random and systematic errors due to the distance errors and the non-uniform sampling. The ways to handle these errors are discussed in [19] and [18], where special attention has been paid to correcting for inhomogeneous Malmquist bias. A degree of freedom remains because the inferred distances are only relative. The mean Hubble flow is tentatively fixed by minimizing velocity residuals within the volume sampled. Therefore, a Hubble-like peculiar velocity error is expeceted, corresponding to a DC offset of order 10% in density fluctuation.

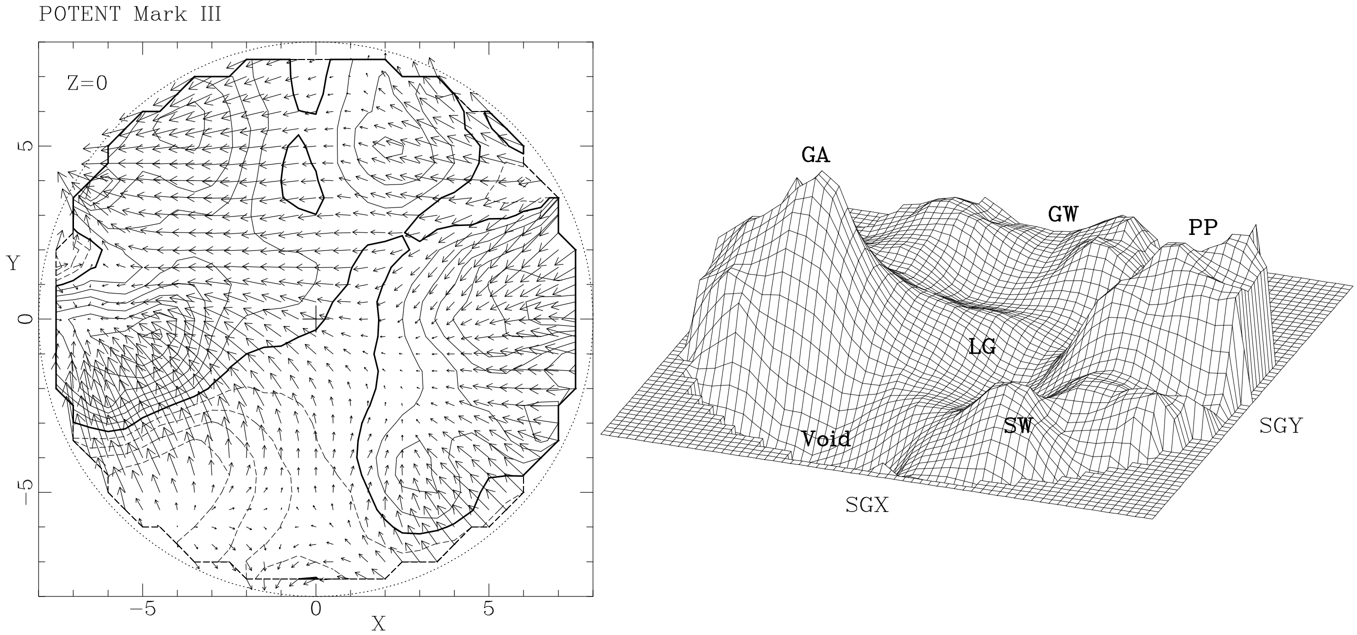

Figure 2: The fluctuation fields of velocity and *mass*-density in the Supergalactic plane as recovered by POTENT from the Mark III velocities of $\sim$ 3000 galaxies with $12\,\mathrm{h}^{-1}$Mpc smoothing. The vectors shown are projections of the 3D velocity field in the CMB frame. Distances and velocities are in 1000 $\mathrm{km\,s}^{-1}$. Contour spacing is 0.2 in δ, with the heavy contour marking $\delta = 0$ and dashed contours $\delta < 0$. The LG is at the center. The GA is on the left, PP on the right, and Coma is at the top. The grey-scale in the contour map and the height of the surface in the landscape map are proportional to δ (Dekel *et al.* 1994).

Three arguments support our working hypothesis that the peculiar velocities are *real* and that they grew by *GI*: (a) the velocity fields traced separately by spirals and by ellipticals, using different distance indicators, are consistent with each other [34], (b) the COBE detection of $\delta T/T \sim 10^{-5}$, and the local bulk velocity of ~ 350 $\mathrm{km\,s}^{-1}$ across $\sim 100\,\mathrm{h}^{-1}$Mpc, are consistent with each other (§5.1 and [7]), and (c) the galaxy density from redshift catalogs and the mass density recovered from observed velocities are consistent with each other [20]. We thus adopt the hypothesis that the velocities are real and generated by the gravity induced by the mass-density fluctuations, and we try to determine Ω from them.

4 Omega from Velocities and Gaussian Fluctuations

4.1 Velocities in Voids

A diverging flow in an extended low-density region can provide a robust dynamical lower bound on Ω, based on the fact that large gravitating outflows are *not* expected in a low-Ω universe [23]. In practice, we assume a value for Ω and use the derivatives of the observed velocity field in diverging regions to infer a non-linear approximation to the mass density there, via the approximation δ_c (5). When the true value of Ω is used, this approximation is typically an overestimate, $\delta_c > \delta$. For fluctuations that started Gaussian, the probability that δ_c is an overestimate, in the range $\delta < -0.5$, is well over 99%. Analogously to $\delta_0 \approx -\Omega^{-0.6}\boldsymbol{\nabla}\cdot\boldsymbol{v}$, the

δ_c inferred from a given diverging velocity field is more negative when a smaller Ω is assumed, and for a small enough Ω it may even be smaller than -1. This provides a lower bound on Ω because mass is never negative and therefore $\delta < -1$ is forbidden.

The inferred δ_c field, smoothed at $12\,h^{-1}$Mpc, and the associated error field σ_δ, were derived by POTENT from the observed radial velocities, and, focusing on the deepest density wells, the assumed Ω was lowered until δ_c became significantly smaller than -1. The most promising "test case" provided by the Mark III data is a broad diverging region centered near the supergalactic plane at the vicinity of $(X, Y) = (-25, -40)$ in h^{-1}Mpc — the "Sculptor void" of galaxies between the GA and the "Southern Wall" extension of PP (Figure 3, compare to figure 2).

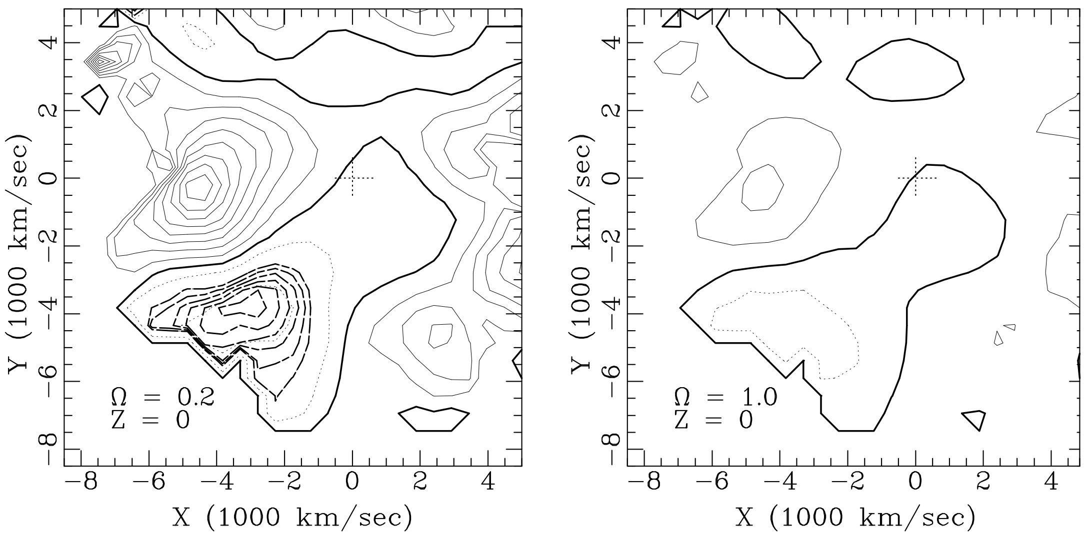

Figure 3: Maps of δ_c inferred from the observed velocities near the Sculptor void in the Supergalactic plane, for two values of Ω. The LG is marked by '+' and the void is confined by the Pavo part of the GA (left) and the Aquarius extension of PP (right). Contour spacing is 0.5, with $\delta_c = 0$ heavy, $\delta_c > 0$ solid, and $\delta_c < 0$ dotted. The heavy-dashed contours mark the illegitimate downward deviation of δ_c below -1 in units of σ_δ, starting from zero (*i.e.* $\delta_c = -1$), and decreasing with spacing -0.5σ. The value $\Omega = 0.2$ is ruled out at the 2.9σ level (Dekel & Rees 1994).

Values of $\Omega \approx 1$ are perfectly consistent with the data, but δ_c becomes smaller than -1 already for $\Omega = 0.6$. The values $\Omega = 0.3$ and 0.2 are ruled out at the 2.4σ and 2.9σ levels in terms of the random error σ_δ.

This result is still to be improved. The systematic errors have been partially corrected in POTENT, but a more specific investigation of the biases affecting the smoothed velocity field in density wells is still in progress. For the method to be effective one needs to find a void that is (a) bigger than the correlation length for its vicinity to represent the universal Ω, (b) deep enough for the lower bound to be tight, (c) nearby enough for the distance errors to be small, and (d) properly sampled to trace the velocity field in its vicinity.

4.2 Skewness of $\nabla \cdot \boldsymbol{v}$

Assuming that the initial fluctuations are a *Gaussian* random field, the one-point probability distribution function (PDF) of smoothed density develops a characteristic skewness due to non-linear effects early in the non-linear regime [33]. The skewness of δ is given according to second-order perturbation theory by

$$\langle\delta^3\rangle/\langle\delta^2\rangle^2 \approx (34/7 - 3 - n) \ , \tag{6}$$

with n the effective power index of the power spectrum near the (top-hat) smoothing scale [9]. Since this ratio of moments for δ is practically independent of Ω, and since $\boldsymbol{\nabla}\cdot\boldsymbol{v} \sim -f\delta$, the corresponding ratio for $\boldsymbol{\nabla}\cdot\boldsymbol{v}$ must strongly depend on Ω, and indeed in second-order it is [**?**]

$$T_3 \equiv \langle(\boldsymbol{\nabla}\cdot\boldsymbol{v})^3\rangle/\langle(\boldsymbol{\nabla}\cdot\boldsymbol{v})^2\rangle^2 \approx -f(\Omega)^{-1}(26/7 - 3 - n) \ . \tag{7}$$

Using N-body simulations and $12\,\mathrm{h}^{-1}$Mpc smoothing one indeed finds $T_3 = -1.8 \pm 0.7$ for $\Omega = 1$ and $T_3 = -4.1 \pm 1.3$ for $\Omega = 0.3$, where the error is the cosmic scatter for a sphere of radius $40\,\mathrm{h}^{-1}$Mpc in a CDM universe ($H_0 = 75$, $b = 1$). An estimate of T_3 in the current POTENT velocity field within $40\,\mathrm{h}^{-1}$Mpc is -1.1 ± 0.8, where the errors this time represent distance errors. With the two errors added in quadrature, $\Omega = 0.3$ is rejected at the $\sim 2\sigma$ level (somewhat sensitive to the assumed PS).

4.3 Initial PDF

Since the present PDF contains only part of the information stored in the data and is in some cases not that sensitive to the initial PDF (IPDF), a more powerful bound can be obtained by using the detailed present velocity field $\boldsymbol{v}(\boldsymbol{x})$ to recover the IPDF, and using the latter to constrain Ω by measuring it's Ω-dependent deviation from the assumed normal distribution [42]. The necessary "time machine" is provided by an Eulerian interpretation of the Zel'dovich approximation [41].

The velocity out of POTENT Mark II, within a conservatively selected volume, was fed into the IPDF recovery procedure with Ω either 1 or 0.3, and the errors due to distance errors and cosmic scatter were estimated. The IPDF recovered with $\Omega = 1$ is found marginally consistent with Gaussian, while the one recovered with $\Omega = 0.3$ shows significant deviations. The largest deviation, bin by bin in the IPDF, is $\lesssim 2\sigma$ for $\Omega = 1$ and $> 4\sigma$ for $\Omega = 0.3$, and a similar rejection of $\Omega = 0.3$ is obtained with a χ^2-type statistic. The skewness and kurtosis are poorly determined because of noisy tails but the replacements $\langle x|x|\rangle$ and $\langle |x|\rangle$ allow a rejection of $\Omega = 0.3$ at the $(5-6)\sigma$ levels!

5 Omega from Velocities and CMB via Power Spectrum

The observed peculiar velocities constrain the amplitude of dynamical fluctuations on scales $\lesssim 100\,\mathrm{h}^{-1}$Mpc, while The fluctuations observed in the CMB by COBE span an angle range corresponding to $\gtrsim 1000\,\mathrm{h}^{-1}$Mpc, comoving, at $z \sim 10^3$. The relation between the two measurements involves Ω via the fluctuation growth rate and the shape (power index n) of the linear power spectrum (PS) on large scales. I describe the acquisition of two related statistics from the peculiar velocities, the bulk velocity and the mass PS, and the conclusions from comparing them with COBE's measurements. The bulk velocity provides a general confirmation of GI for $n \sim 1$, while the PS is a more sensitive measure of Ω.

5.1 Bulk Velocity

A robust statistic that is relatively straightforward to obtain is the bulk velocity V within a sphere of radius R centered on the LG. It is computed, for example, by volume-weighted vector averaging of the smoothed peculiar velocities computed by POTENT at grid points [6] . Alternatively, it is obtained by minimizing the residuals of the observed radial peculiar velocities from a bulk velocity across the sphere [14].

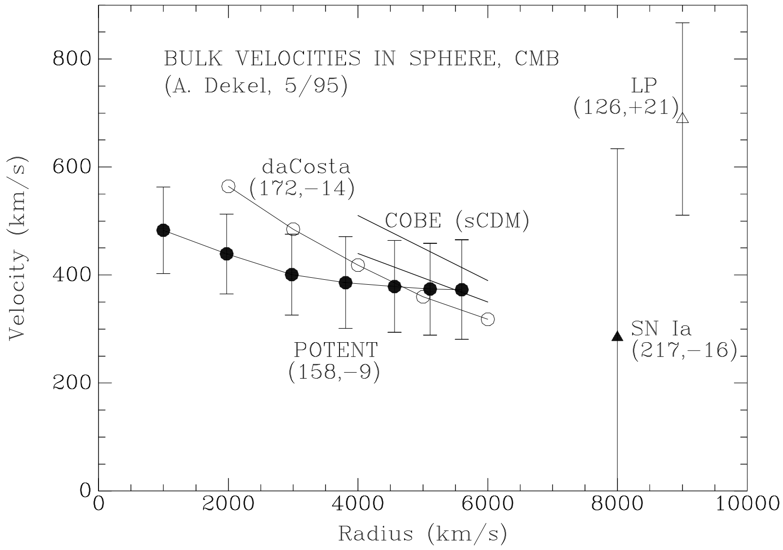

Figure 4: The amplitude of the bulk velocity relative to the CMB frame, in top-hat spheres about the LG. The directions are indicated in supergalactic coordinates (L, B).

The amplitude of the bulk velocity as a function of R, from several recent sources, is shown in Figure 4. The Mark III POTENT result [25] at $R = 50\,\mathrm{h}^{-1}$Mpc is $V = 374 \pm 85$ km s^{-1} towards $(L, B) = (158°, -9°) \pm 10°$. The $\sim$20% error bars are due to distance errors, and one should consider an additional uncertainty of similar magnitude due to non-uniform sampling. Another sample of Sc galaxies by daCosta *et al.* [16] yields at the same R a very similar result (contrary to premature rumors), $V \approx 364$ km s^{-1} towards $(172°, -14°)$ [although the slope of the $V(R)$ curve is somewhat steeper in this, still preliminary, analysis]. Within a larger sphere of $R \sim 100\,\mathrm{h}^{-1}$Mpc, the bulk velocity based on Type Ia supernovae [46] is $V = 284 \pm 350$ km s^{-1} (consistent with zero!) towards $(217°, -16°) \pm 70°$. This measurement is based on only 13 distances, but the claimed errors of only $\sim$5% enable a meaningful result. This new large-scale result fits nicely any natural extrapolation of the POTENT results from smaller scales, and they all make a bulk of sense within the framework of standard isotropic and homogeneous cosmology.

The only apparently discrepant result comes from the velocities measured on a similar large scale using brightest cluster galaxies (BCG) as distance indicators ([37], LP), which show a large bulk velocity of $V = 689 \pm 178$ towards a very different direction $\sim (126, 21)$. An ongoing effort to measure a larger sample of clusters will soon tell whether this early result is a $\gtrsim 2\sigma$ statistical fluke [27], whether the errors were underestimated, or whether something is systematically different between the BCG distances and the distances measured by other indicators. Until then, it would make sense to put this result on hold.

Shown in comparison are the expected *rms* bulk velocity in a standard CDM model ($\Omega = 1$, $n = 1$) normalized to COBE, for $h = 0.5$ (bottom) and 0.8 (top) [50]. These theoretical curves would not change much if a 20% hot component is mixed with the cold dark matter, or if Ω is lower but still in the range $0.2 - 1.0$, as long as $n \approx 1$. When compared to a theoretical prediction, the error should also include cosmic scatter due to the fact that only one sphere has been sampled from a random field. These errors are typically on the order of the measurement errors.

The CMB fluctuations on scales $\leq 90^\circ$ are of course independent of the local motions, but GI theory predicts an intimate relation between them, which can serve as a basic test for GI. The CMB fluctuations are associated with fluctuations in gravitational potential in the surface of last scattering at $z \sim 10^3$, while their sister fluctuations in our neighborhood have grown by gravity to produce the motions observed. The local surveyed region of $\sim 100\,\mathrm{h}^{-1}$Mpc corresponds to a $\sim 1^\circ$ patch on the last-scattering surface of some hypothetical distant observer. The major effect on scales $> 1^\circ$ is the Sachs-Wolfe effect, where potential fluctuations $\Delta\Phi_g$ induce temperature fluctuations via gravitational redshift, $\delta T/T = \Delta\Phi_g/(3c^2)$. Since the velocity potential is proportional to Φ_g in the linear and quasi-linear regimes, and since linear potential fluctuations do not grow in comoving coordinates, one can write $\Delta\Phi_g \propto Vx$, where x is the scale across which the bulk velocity is V. A typical bulk velocity of ~ 300 km s^{-1} across $\sim 100\,\mathrm{h}^{-1}$Mpc corresponds to $\delta T/T \sim 10^{-5}$ at $\sim 1^\circ$. If the fluctuations are roughly scale-invariant ($n \approx 1$), then $\delta T/T \sim 10^{-5}$ is expected on all scales above 1°. Several years ago we drew [7] a $\delta T/T$ map of the local GA-PP region as seen by a distant observer, and predicted $\delta T/T \sim 10^{-5}$. Now that such CMB fluctuations have been detected in the range $1^\circ - 90^\circ$ ([48], [47]), they provide an important confirmation of GI, truly addressing the specific *growth rate* of structure as predicted by this theory [2].

The COBE-normalized bulk flow as predicted by theory depends on n but is not that sensitive to Ω or to the nature of the dark matter (DM). The main effect of Ω and H_0 on the PS is via the location of the peak, at $k_{peak} \sim 0.065(\Omega h)^{-1}(\mathrm{h}^{-1}\mathrm{Mpc})^{-1}$, corresponding to the horizon scale at the epoch of equal energy densities in matter and radiation. The DM type mostly affects the shape of the filtered PS at larger k's. The predicted bulk velocity over $\sim 100\,\mathrm{h}^{-1}$Mpc is efectively an integral of the PS over wavenumbers smaller than k_{peak}, and is therefore relatively insensitive to Ω while it is quite sensitive to n. From the bulk velocity by POTENT at $R = 50\,\mathrm{h}^{-1}$Mpc, we obtain for $\Omega = 1$ CDM with no tensor fluctuations that $n \simeq 0.55 h_{50}^{-0.94} \pm 0.3$.

5.2 Mass Power Spectrum from POTENT

The local PS, at $k > k_{peak}$ where the PS is steep, should be more sensitive than the bulk velocity to Ωh (or a similar combination). In a recent work (Kolatt & Dekel [35]), we have derived the PS from the smoothed Mark III POTENT density field, and compared to COBE to yield Ωh and n.

There is a long way between the true fluctuation signal and the observed PS. The data is contaminated by distance errors, and sampled sparsely and non-uniformly. It is then smoothed heavily and is subjected to the POTENT analysis where quasilinear approximations are used to derive the density field and the associated errors on a uniform grid. The density field is taken from within a window of effective radius $\sim 50\,\mathrm{h}^{-1}$Mpc, weighted inverseley by the squares of the local errors, and zero-padded in a larger periodic box before an FFT procedure is applied and the PS is computed by averaging the amplitides of the Fourier transforms in bins of k. Term the product "the observed PS", $O(k)$.

The systematic errors introduced by the above procedure are modeled by

$$O(k) = M(k)[S(k) + N(k)], \tag{8}$$

where $S(k)$ is the true signal PS, $N(k)$ is the noise PS, and $M(k)$ represents the effects of sampling, smoothing, applying a window etc. The correction functions $M(k)$ and $N(k)$ are derived from Monte Carlo mock catalogs based on simulations that mimic in detail the underlying structure of the real universe and the Mark III catalog [36]. The factor $M(k)$ is derived first by $M^{-1} = S/\langle O\rangle_{no-noise}$, where S here is the known signal PS built into the simulations, and the averaging is over 10 mock catalogs not perturbed by noise. Then $N(k)$ is computed by $N = M^{-1}\langle O\rangle_{noise} - S$, where the averaging this time is over noisy mock catalogs.

Equipped with the correction functions $M(k)$ and $N(k)$, the PS observed from the real universe, $O(k)$, is finally corrected to yield the true PS by

$$S(k) = M(k)^{-1}O(k) - N(k). \tag{9}$$

The recovered mass-density PS is shown in Figure 5 using three thick logarithmic bins covering the range $0.04 \le k \le 0.2\,(\mathrm{h}^{-1}\mathrm{Mpc})^{-1}$, within which the results are reliable. For example, we find $P(k)f(\Omega)^2 = (4.6 \pm 1.4) \times 10^3(\mathrm{h}^{-1}\mathrm{Mpc})^3$ at $k = 0.1(\mathrm{h}^{-1}\mathrm{Mpc})^{-1}$ (using the convention where the Fourier transform is defined with no 2π factors in it's coeficient).

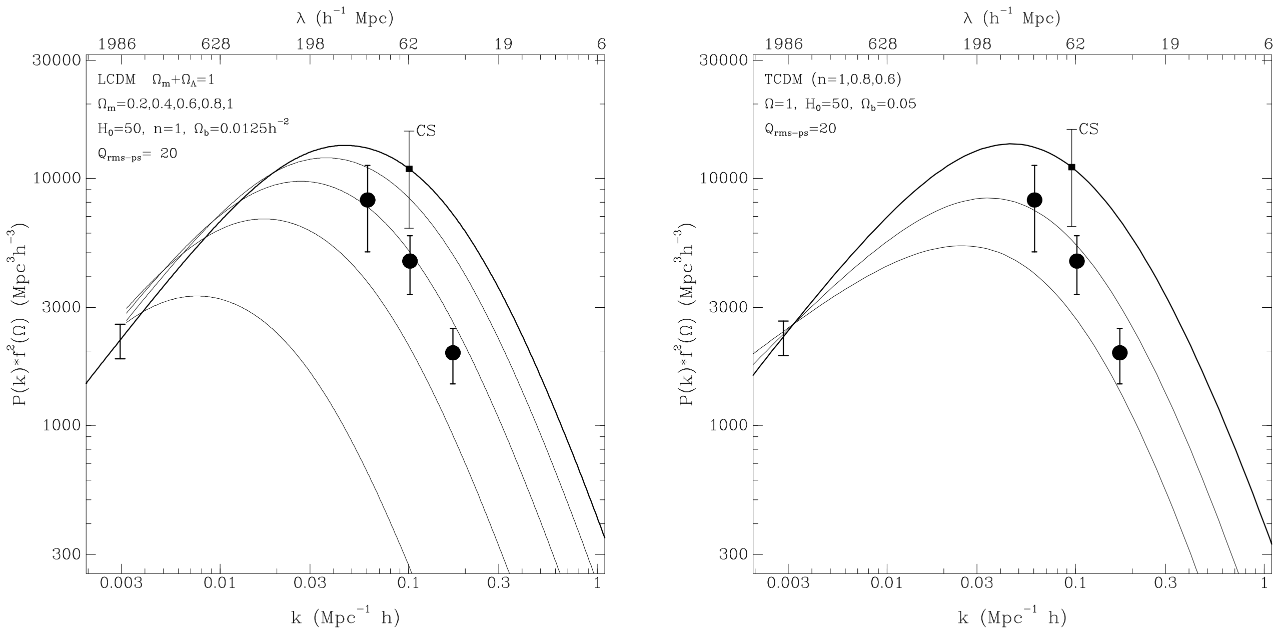

Figure 5: The mass power spectrum $[\times f(\Omega)^2]$ from Mark III POTENT velocities (circles), with 1σ random errors. The curves are COBE-normalized theoretical predictions for flat CDM with $h = 0.5$. Left: $n = 1$ and Ω growing upeards. Right: $\Omega = 1$ and n growing upwards. Cosmic scatter for $\Omega = 1$ and $n = 1$ is indicated (square).

The observed PS is compared in the figure to the linear predictions of a family of Inflation-motivated flat ($\Omega + \Lambda = 1$) CDM models with the Hubble constant arbitrarily fixed at $h = 0.5$. For $n = 1$, maximum likelihood is obtained at $\Omega \simeq 0.55h_{50}^{-1.35} \pm 0.1$. For $\Omega = 1$, assuming that tensor fluctuations do not contaminate the fluctuations observed by COBE, the linear power index is $n \simeq 0.70h_{50}^{-0.8} \pm 0.1$.

5.3 Mass Power Spectrum from Likelihood Analysis

The PS, in a parametric form including Ω, h and n among the parameters, has alternativelly been determined from the velocity data via a Baysian likelihood analysis (Zaroubi, Dekel & Hoffman [56]). According to Bayse, the probability of the model parameters given the data, which is the function one wishes to maximize, can be expresses as

$$P(model|data) = P(data|model)\, P(model)/P(data). \tag{10}$$

$P(data)$ serves here as a normalization constant. Without any external constraints on the model parameters, one assumes that $P(model)$ is a constant in a given range. The remaining task is to maximize the likelihood as a function of the model parameters, $L = P(data|model)$, which is easier to write down explicitly.

Under the assumption that the velocities and the errors are both Gaussian random fields with no mutual correlations, the likelihood can be written as

$$L = (2\pi|D|)^{-1/2} \exp(-d_i D_{ij}^{-1} d_j/2), \tag{11}$$

where d_i are the data at points $i = 1, ..., N$, and D_{ij} is the covariance matrix, which one can split into covariance of signal (s) and covariance of noise (n),

$$D_{ij} \equiv \langle d_i d_j \rangle = \langle s_i s_j \rangle + \langle n_i n_j \rangle. \tag{12}$$

If the errors are uncorrelated, the noise matrix is diagonal. The signal matrix is computed from the model PS, and is therefore a function of the desired model parameters.

We used a parametric model for the PS of the general form

$$P_k = A\, k^n\, T(\Gamma_i; k), \tag{13}$$

where $T(k)$ is a small-scale filter of an assumed shape characterized by free parameters Γ_i, k^n is the initial PS, which is still valid on large scales today, and A is a normalization factor. The normalization can either be determined by COBE's data (for given Ω, Λ, h, n and tensor/scalar fluctuations), or be left as a free parameter to be fixed by the velocity data alone. The filter $T(k)$ can be taken from a specific physical model (e.g. CDM, where $\Gamma = \Omega h$ [17]), or be an arbitrary function with enough flexibility to fit the data.

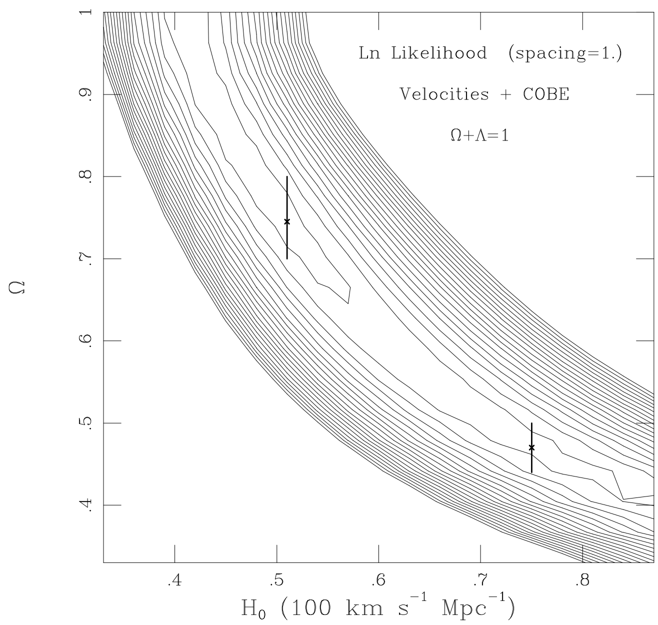

Figure 6: Likelihood contour map in the $\Omega - h$ plane, for flat CDM with $n = 1$. Marked are the most likely values of Ω and the corresponding 1σ error bars for two given values of h.

This likelihood analysis yields for flat CDM with $n = 1$, $\Omega \simeq (0.75 \pm 0.05) h_{50}^{-1.2}$. For $\Omega = 1$ CDM with no tensor fluctuations, $n \simeq (0.90 \pm 0.04) h_{50}^{-0.8}$, and with tensor fluctuations $n \simeq (0.95 \pm 0.02) h_{50}^{-0.8}$.

Focusing on the shape of the PS as constrained by the velocities alone without COBE's normalization, maximum likelihood for a CDM-like filter is obtained with a shape parameter $\Gamma = 0.50 \pm 0.12$, but note that here Γ is not directly related to the cosmological parameters

Ω and h. The normalization as determined for this PS shape can be expressed by $P[k = 0.1(hmpc)^{-1}] = (4.1 \pm 0.6) \times 10^3 (hmpc)^3$, or alternatively by the dispersion in top-hat spheres of radius $8\,\mathrm{h}^{-1}\mathrm{Mpc}$, $\sigma_8 = 0.8 \pm 0.12$.

Both Ω and n obtained by the likelihood analysis of this section tend to be slightly higher than their estimates based on the PS recovered from the POTENT output in the previous section §5.2. The errors quoted from the likelihood analysis, unlike the errors quoted in the previous section, do not include cosmic scatter. The difference between the results obtained in the two different ways is on the order of the errors in each analysis and the cosmic scatter. Our tentative best guess should probably be a crude average of the two results.

6 Summary

My goal in this paper has been to demonstrate that there are several ways to constrain Ω from dynamical measurements of large-scale structure *independently* of galaxy biasing. The current data enable us to reject values of Ω as low as 0.3 at the 95-99% confidence level in several different ways.

Figure 7 puts our results in perspective, in terms of the ongoing general discussion concerning the cosmological parameters. Shown are various limits derived from observations, on top of theoretical curves relating the age of the universe to the Hubble constant for a given value of Ω, as predicted for the Inflation-motivated family of flat cosmological models.

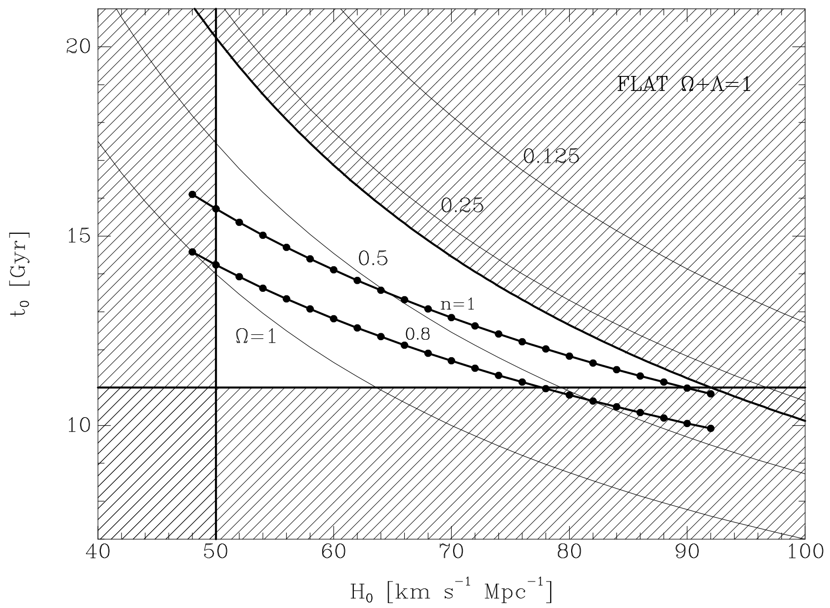

Figure 7: Constraints on the cosmological parameters.

I adopt $\sim 2\sigma$ lower bounds of $h > 0.5$ [45] and $t_0 > 11\,\mathrm{Gyr}$ ([8], [32]). Combined with the limit reported here with similar confidence, of $\Omega > 0.3$, the parameters are confined to a concordence "triangle".

The results of combining the peculiar velocity data with COBE's $\delta T/T$ via the mass-density power spectrum, assuming CDM, are shown as dotted lines for $n = 1$ and for $n = 0.8$ (no tensor fluctuations).

If h is indeed as high as $0.7 - 0.8$, as indicated by recent cepheid measurements [28], then Ω seems to be confined to 0.5 ± 0.2, and then CDM with $n = 1$ could provide an appropriate spectrum. If it turns out that h is only about $0.5 - 0.6$, then an $\Omega = 1$ CDM model becomes a viable option, provided that n is somewhat smaller than unity, perhaps associated with a nonzero component of tensor fluctuations.

Acknowledgements. Parts of the work described above have been done together with different collaborators, including Bernardeau, Buchet, Burstein, Courteau, Faber, Hoffman, Juszkieicz, Kolatt, Lahav, Nusser, Rees, Willick, and Zaroubi. Parts of this work were supported by the Israel Science Foundation and by the US-Israel Binational Science Foundation.

References

[1] Aaronson, M., Huchra, J., Mould, J.R., Tully, R.B., Fisher, J.R., *et al.* 1982a, *Ap. J. Supp.* **50**, 241.

[2] Babul, A., Weinberg, D., Dekel, A., & Ostriker, J.P. 1994, *Ap. J.* **427**, 1

[3] Bardeen, J., Bond, J.R., Kaiser, N. & Szalay, A. 1986, *Ap. J.* **304**, 15

[4] Bernardeau, F., Juszkiewicz, R., Bouchet, F., & Dekel, A. 1995, *Ap. J.* **,** *in press*

[5] Bertschinger, E., & Dekel, A. 1989, *Ap. J. Lett.* **336**, L5

[6] Bertschinger, E., Dekel, A., Faber, S.M., Dressler, A., & Burstein, D. 1990, *Ap. J.* **364**, 370

[7] Bertschinger, E., Gorski, K., & Dekel, A. 1990, *Nature* **345**, 507

[8] Bolte, M. & Hogan, C.J. 1995, *Nature* **,** *submitted*

[9] Bouchet, F., Juszkiewicz, R., Colombi, S., & Pellat, R. 1992, *Ap. J. Lett.* **394**, L5

[10] Braun, E., Dekel, A., & Shapiro, P. 1988, *Ap. J.* **328**, 34

[11] Burstein, D. 1990, *Distributed electronically*

[12] Cen, R., & Ostriker, J.P. 1992, *Ap. J.* **399**, L113

[13] Cen, R., & Ostriker, J.P. 1993, *Ap. J.* **417**, 415

[14] Courteau, S., Faber, S.M., Dressler, A., & Willick, J.A. 1993, *Ap. J. Lett.* **412**, L51

[15] Courteau, S. 1992, *Ph.D. Thesis, UCSC*

[16] daCosta, L. *et al.* , in Cosmic Velocity Fields, eds. F Bouchet & M. Lachieze-Rey (Editions Frontieres)

[17] Davis, M., Efstathieou, G., Frenk, C.S., & White, S.D.M. 1985, *Ap. J.* **292**, 371

[18] Dekel, A. 1994, *Annu. Rev. Astron. Astrophys.* **32**, 371

[19] Dekel, A., Bertschinger, E., & Faber, S.M. 1990, *Ap. J.* **364**, 349

[20] Dekel, A., Bertschinger, E., Yahil, A., Strauss, M., Davis, M., & Huchra, J. 1993, *Ap. J.* **412**, 1

[21] Dekel, A. & Lahav, O. 1996, *in preparation*

[22] Dekel, A. & Rees, M.J. 1987, *Nature* **326**, 455

[23] Dekel, A. & Rees, M.J. 1994, *Ap. J. Lett.* **422**, L1

[24] Dekel, A., & Silk, J. 1986, *Ap. J.* **303**, 39

[25] Dekel *et al.* 1996, *Ap. J.* , *in preparation*

[26] Dressler, A. 1980, *Ap. J.* **236**, 351

[27] Feldman, H.A., & Watkins, R. 1995, *preprint*

[28] Freedman, W. *et al.* 1994, *Nature* **371**, 757

[29] Han, M.S. & Mould, J.R. 1990, *Ap. J.* **360**, 448

[30] Han, M.S. & Mould, J.R. 1992, *Ap. J.* **396**, 453

[31] Hudson, M.J., Dekel, A., Courteau, S., Faber, S.M., & Willick, J.A. 1995, *MNRAS* **274**, 305

[32] Jimenez, R. *et al.* 1995, *submitted*

[33] Kofman, L., Bertschinger, E., Gelb, J., Nusser, A., & Dekel, A. 1994, *Ap. J.* **420**, 44

[34] Kolatt, T. & Dekel, A. 1994a, *Ap. J.* **428**, 35

[35] Kolatt, T. & Dekel, A. 1996, *in preparation*

[36] Kolatt, T., Dekel, A., Ganon, G., & Willick, J. 1996, *Ap. J.* , *submitted*

[37] Lauer, T.R., & Postman, M. 1994, *Ap. J.* **425**, 418

[38] Lynden Bell, D., Faber, S.M., Burstein, D., Davies, R.L., Dressler, A., Terlevich, R. J., & Wegner, G. 1988, *Ap. J.* **326**, 19

[39] Mathewson, D.S., Ford, V.L., & Buchhorn, M. 1992, *Ap. J. Supp.* **81**, 413

[40] Mould, J.R. *et al.* 1991, *Ap. J.* **383**, 467

[41] Nusser, A. & Dekel, A. 1992, *Ap. J.* **391**, 443

[42] Nusser, A. & Dekel, A. 1993, *Ap. J.* **405**, 437

[43] Nusser, A., Dekel, A., Bertschinger, E., & Blumenthal, G.R., 1991, *Ap. J.* **379**, 6

[44] Nusser, A., Dekel, A., & Yahil, A. 1995, *Ap. J.* , *in press*

[45] Press, W. 1995, in *Unsolved Problems in Astrophysics* ed. D. Spergel (Princeton University Press)

[46] Riess, A.G., Press, W.H., & Kirshner, R.P. 1995, *Ap. J. Lett.* **438**, L17

[47] Schuster, J. *et al.* 1993, *Ap. J. Lett.* , in press

[48] Smoot, G.F. *et al.* 1992, *Ap. J. Lett.* **396**, L1

[49] Strauss, M. & Willick, J. 1995, Physics Reports, *in press*

[50] Sugiyama, N. 1995, *Ap. J. in press*

[51] Weinberg, D. 1995, in Wide-Field Spectroscopy and the Distant Universe, eds. S.J. Maddox & A. Aragon-Salamanca (World Scientific: Singapore)

[52] Willick, J. 1991, *Ph.D. Thesis, UC Berkeley*

[53] Willick, J.A., Courteau, S., Faber, S.M., Burstein, D., & Dekel, A. 1995, *Ap. J.* , *in press.*

[54] Willick, J.A., Courteau, S., Faber, S.M., Burstein, D., Dekel, A. & Kolatt, T. 1996a, *Ap. J.* , *submitted.*

[55] Willick, J.A., Courteau, S., Faber, S.M., Burstein, D., & Dekel, A. 1995, *Ap. J. Supp.* , *in preparation*

[56] Zaroubi, S., Dekel, A., & Hoffman, Y. 1996, *in preparation*